TU Delft

Delft University of Technology

New insights into autogenous self-healing in cement paste based on nuclear magnetic resonance (NMR) tests

Huang, Haoliang; Ye, Guang; Pel, Leo

DOI
10.1617/s11527-015-0664-9

Publication date
2016

Document Version
Final published version

Published in
Materials and Structures

Citation (APA)
Huang, H., Ye, G., & Pel, L. (2016). New insights into autogenous self-healing in cement paste based on nuclear magnetic resonance (NMR) tests. *Materials and Structures*, *49*(7), 2509-2524. https://doi.org/10.1617/s11527-015-0664-9

Important note
To cite this publication, please use the final published version (if applicable).
Please check the document version above.

Copyright
Other than for strictly personal use, it is not permitted to download, forward or distribute the text or part of it, without the consent of the author(s) and/or copyright holder(s), unless the work is under an open content license such as Creative Commons.

Takedown policy
Please contact us and provide details if you believe this document breaches copyrights.
We will remove access to the work immediately and investigate your claim.

This work is downloaded from Delft University of Technology.
For technical reasons the number of authors shown on this cover page is limited to a maximum of 10.

Materials and Structures (2016) 49:2509–2524
DOI 10.1617/s11527-015-0664-9

ORIGINAL ARTICLE

New insights into autogenous self-healing in cement paste based on nuclear magnetic resonance (NMR) tests

Haoliang Huang · Guang Ye · Leo Pel

Received: 30 December 2014 / Accepted: 29 June 2015 / Published online: 10 July 2015
© RILEM 2015

Abstract The aim of this study is to investigate the effect of water migration from cracks into the bulk paste on autogenous self-healing. Nuclear magnetic resonance (NMR) technique was utilized to monitor water migration from cracks into the bulk paste during the process of autogenous self-healing. NMR results show that initially the water in the crack migrates into the bulk paste and the water content of the bulk paste increases significantly. However, after 5-h autogenous self-healing, the amount of non-chemically bound water in the bulk paste (adjacent to the crack surfaces) determined by NMR decreased instead. It indicates that some of the water coming from the crack was used for additional hydration of unhydrated cement particles in the bulk paste (during the process of autogenous self-healing). Before this study, in term of autogenous self-healing only the recoveries that related to the filling of cracks were concerned. The observation and quantification of densification of cement paste adjacent to the crack surfaces provides a new insight into autogenous self-healing.

Keywords Nuclear magnetic resonance (NMR) · Autogenous self-healing · Water migration · Additional hydration · Cement paste

H. Huang (✉)
School of Materials Science and Engineering, Southeast University, Nanjing 211198, China
e-mail: h.l.huang@msn.com

H. Huang · G. Ye
Department of Civil Engineering and Geoscience, Delft University of Technology, 2628 CN Delft, The Netherlands

G. Ye
Department of Structural Engineering, Ghent University, 9052 Ghent, Belguim

L. Pel
Department of Applied Physics, Eindhoven University of Technology, 5600 MB Eindhoven, The Netherlands

1 Introduction

Concrete is a brittle composite cementitious material that easily fractures under tensile loading. Microcracks can appear throughout the concrete prior to application of any load because of temperature-induced strain and autogenous and drying shrinkage [1]. There is no doubt that these cracks provide preferential access for aggressive agents to penetrate into the concrete, probably causing corrosion of reinforcement steel and degradation of concrete. As a result, the service life of reinforced concrete structures is shortened.

Self-healing of cracks has a significant potential to extend the service life of reinforced concrete structures [2, 3, 4, 5, 6, 7, 8]. The self-healing process was defined as autonomous healing when the recovery process uses materials components that are specially design for self-healing [9]. Actually, even though

without any added healing agents, it was found that concrete still has the ability to heal its cracks [10, 11]. This ability was defined as autogenous self-healing [10, 11]. Autogenous self-healing in Portland cement concrete has attracted much attention since it was observed many years ago. According to Hearn [12], the phenomena of autogenous self-healing had already been noticed in water retaining structures, culverts and pipes by Hyde and Smith [13] by the end of nineteenth century. In 1920s, a more systematical analysis of autogenous self-healing was executed by Glanville [14].

In recent years, autogenous self-healing was investigated extensively [15, 16], Lv and Chen [17]. Yang et al. [18] and Qian et al. [19] conducted tensile tests and bending tests to study the self-healing efficiency in ECC. Granger et al. [20] estimated the efficiency of self-healing in high strength concrete by performing three-point bending tests in combination with acoustic emission analysis. Heide [21] also carried out three-point bending tests to evaluate self-healing in concrete. They found that the mechanical properties of materials recover, to some extent, after autogenous self-healing of cracks. Edvardsen [22] performed water permeability tests to estimate the efficiency of autogenous self-healing as a function of time. Autogenous self-healing of cracks in high-strength concrete as a function of crack width was evaluated by means of water permeability tests by Reinhardt and Jooss [23]. It was found that after autogenous self-healing water permeability of the materials decreases significantly. In the aforementioned studies, the recovery of material functions after autogenous self-healing depends on the formation of reaction products in cracks, i.e. filling of cracks with reaction products. It is believed that further hydration of unhydrated cement particles is one of the reasons of autogenous self-healing [24, 25, 20, 26]. Dissolution of original hydration products, i.e. portlandite, in the bulk paste and re-deposition of these products in cracks also contribute to autogenous self-healing [24, 26]. Formation of calcite in cracks is one of mechanisms of autogenous self-healing as well [27, 22, 28, 19, 29]. In these processes, water is one of the most essential factors. On the one hand water in cracks serves as a reactant and on the other hand as a medium in which reaction products can precipitate. If cement paste is not saturated with water, in the healing process the water in the crack can migrate into the bulk paste. However, by now the effect of migration of water from cracks into the bulk paste on autogenous self-healing is still not clear yet.

In this study, nuclear magnetic resonance (NMR) was utilized to investigate water migration from cracks into the bulk paste during the process of autogenous self-healing. The changes of water content and water distribution in the bulk paste adjacent to the crack surfaces were quantified by NMR. By performing NMR tests, a phenomenon in the process of autogenous self-healing was noticed. The effect of water migration (from cracks into the bulk paste) on autogenous self-healing was analyzed.

2 Material and specimen preparation

2.1 Material

The material used in this study was Portland cement paste made of CEM I 42.5 N. The chemical composition and mineral composition of Portland cement CEM I 42.5 N are shown in Tables 1 and 2, respectively. The water to cement ratio (w/c) of the cement paste was 0.3.

2.2 Specimens prepared for NMR tests

In this study, prismatic specimens with a dimension of 20 mm × 20 mm × 145 mm were cast. After casting, the specimen was cured under sealed conditions in a storage with a temperature of 20 ± 1 °C and relative humidity of 50 %. As shown schematically in Fig. 1a, a glass tube with an outside diameter of 4 mm and a wall thickness of 0.7 mm was embedded inside the specimen for delivering extra water (i.e. the water supplied to the sample after cracking) to the crack for autogenous self-healing.

At the age of 40 days, the specimen was loaded in three-point bending until two pieces were obtained (see Fig. 1b). The two pieces of the broken specimen were pressed together from both ends in axial direction (the width of the crack obtained was about 0.5 mm) and glued at the outside with a high viscosity epoxy. Moreover, the surfaces of the cracked specimens were sealed with the same epoxy except both end surfaces (see Fig. 1b). The viscosity of the epoxy was high enough to ensure that the epoxy did not penetrate into the crack (some specimens were cut and checked to make sure that no epoxy had penetrated into the

Table 1 Chemical composition of Portland cement (CEM I 42.5 N)

Compound	CaO	SiO_2	Al_2O_3	Fe_2O_3	K_2O	Na_2O	SO_3	MgO	Total
Weight (%)	64.40	20.36	4.96	3.17	0.64	0.14	2.57	2.09	98.33

Table 2 Mineral composition of Portland cement (CEM I 42.5 N) based on Bogue equation [45]

Compound	C_3S	C_2S	C_3A	C_4AF	Total
Weight (%)	64	13	8	9	94

crack). After the epoxy got hardened, the specimen was ready for the tests.

At the age of 42 days, extra water was delivered to the crack via the glass tube. When the glass tube was filled with water, the water in the glass tube easily penetrated into the crack and induced autogenous self-healing.

3 NMR experiment

3.1 NMR principle

Nuclear magnetic resonance (NMR) is a non-destructive technique for quantitatively mapping certain elements. During an NMR experiment the magnetic moments of the nuclei are manipulated by suitably chosen radio frequency fields [30]. The resonance condition for the nuclei is given as [30]:

$$f = \gamma B_0, \tag{1}$$

where f is the frequency of the alternating field, γ is the gyromagnetic ratio of the nuclei, and B_0 is the magnitude of the externally applied static magnetic field. According to the resonance condition, the measurement can be made only sensitive to hydrogen ($\gamma = 42.58$ MHz/T for ^{1}H) and thereby water [31].

In an NMR equipment, the magnetic moments of hydrogen nuclei are manipulated by suitably chosen alternating radio frequency fields, leading to a so called spin-echo signal [32]. In order to get the maximum signal intensity from the sample before significant relaxation, the signal is acquired as quickly as possible. In this case, the amplitude of this spin-echo signal is proportional to the amount of hydrogen nuclei excited by the radio frequency field [31]. As a result, the amount of water can be quantified.

The spin-echo signal also gives information about the rate at which this magnetic excitation of the spins decays [33]. The system will return to its magnetic equilibrium by two mechanisms: interactions between the nuclei themselves, causing the so-called spin–spin relaxation, and interactions between the nuclei and their environment, causing the so-called spin–lattice relaxation [34]. Assuming that both mechanisms give rise to a single exponential relaxation and that spin lattice relaxation is much slower than the spin–spin relaxation, the magnitude of the NMR spin-echo signal is given [35]:

$$S = \rho \exp\left(-\frac{t_E}{T_2}\right)\left[1 - \exp\left(-\frac{t_R}{T_1}\right)\right], \tag{2}$$

where ρ is the proton density, T_1 is the spin–lattice relaxation time, t_R is the repetition time of the spin-echo experiment, T_2 is the spin–spin or transverse relaxation time and t_E is the so-called spin-echo time. Obviously small T_2 values lead to a decrease of the spin-echo signal. On the other hand, small T_1 values are preferred, as this parameter limits the repetition time (usually $t_R \approx 4T_1$) and hence the rate at which the moisture profiles can be scanned.

By Brownstein–Tarr it was shown that the T_1 and T_2 of water in pores of a material can be related to the pore size [35]. Hence in the case of concrete the total signal is given by:

$$S = \rho \sum_{i=1} \exp\left(-\frac{t_E}{T_{2,1}}\right)\left[1 - \exp\left(-\frac{t_R}{T_{1,i}}\right)\right], \tag{3}$$

where we can sum over the water both in gel and capillary pores. Hence by choosing the appropriate set of t_E and t_R we can select to measure all the water present in gel and capillary pores or just the water present in the gel pores [36]. In this study the moisture profiles were measured with the shortest spin-echo time $t_E = 180$ μs and a variable repetition time. In order to discriminate the water in gel, capillary pores and in the cracks, we have used a variable repetition

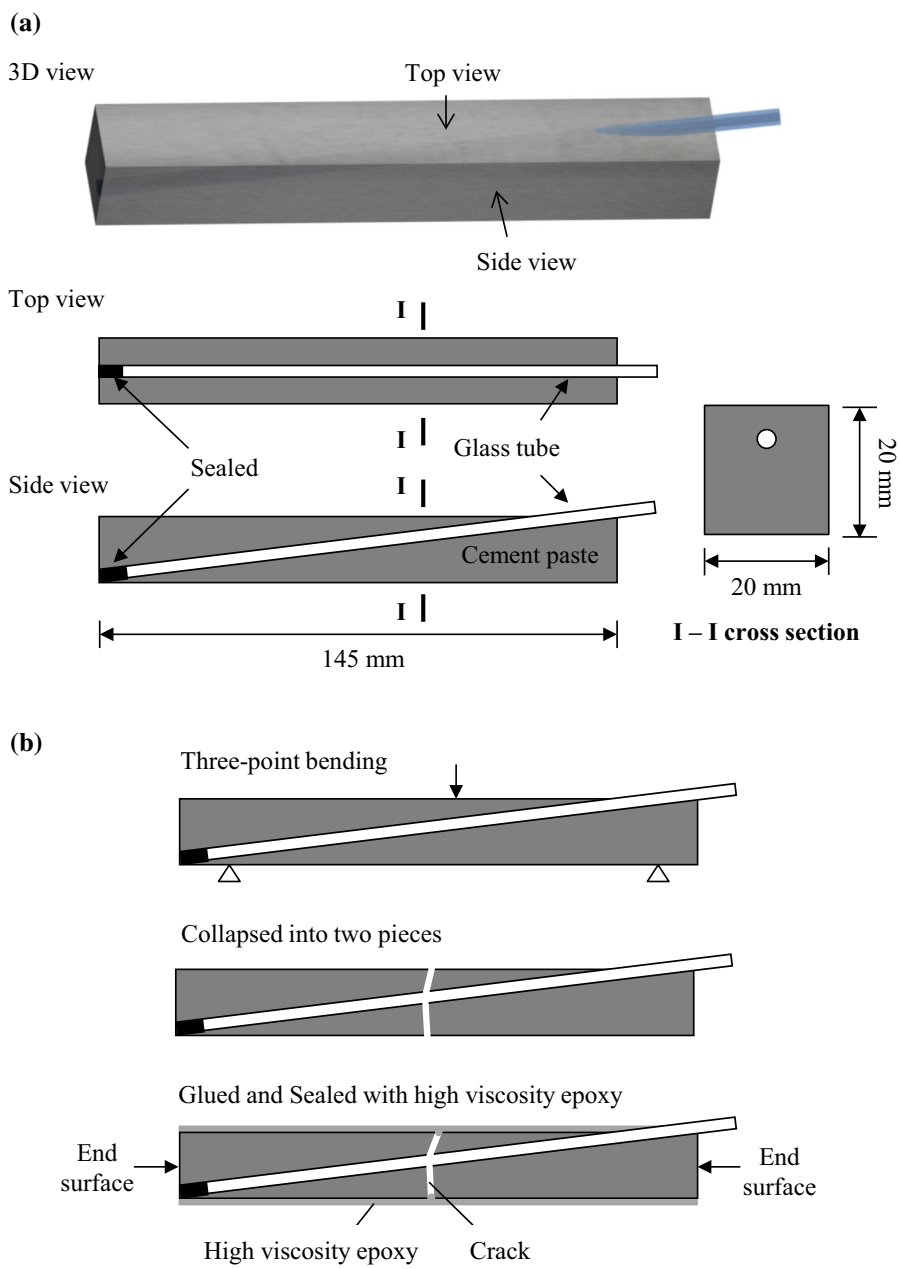

Fig. 1 A schematic diagram of the specimen for the NMR experiment. **a** Specimen before cracking **b** preparation of the cracked specimen for NMR tests

time t_R. Here we have chosen the repetition time based on the measured spin–lattice relaxation times for both the gel and larger capillary pores. The total moisture profiles were measured using a repetition time about four times the longest spin–lattice relaxation time, i.e., the relaxation time of the capillary pores. Hence the moisture profile reflects the total moisture content in both gel and capillary pores. In the other case we have chosen the repetition time to be three times the gel spin–lattice repetition time. In this case the moisture profile will predominantly be determined by the gel moisture content, whereas moisture in larger capillary pores will only give a minor contribution.

3.2 NMR setup

In this study, an NMR setup was used which is especially designed for quantitative moisture measurements in

building materials (see Fig. 2). A Faraday shield was placed between the radio frequency (RF) coil and the sample holder. The use of a Faraday shield was to suppress the effects of the changes of the dielectric permittivity by variations of the water content, thereby making the NMR measurements quantitative [37, 38]. In order to measure a moisture profile, the sample can be moved through the NMR with the help of a stepper motor.

The gradient used in this setup has a strength of 14 kHz/mm, i.e., 0.3 T/m. As a result the 1D resolution of the NMR measurement is in the order of 1 mm. Hence a point measurement here represents the average at one point over a 1 mm slice.

3.3 Calibration

In order to quantify the amount of non-chemically bound water in the sample, the NMR signal against the water content of the sample was calibrated. The initial weight of a specimen at the age of 42 days was measured first (the specimen was not coated and cracked). The signal of the water profile of the specimen was measured by NMR as well. After that, the specimen was submersed completely in water. After absorbing water for a certain time, the sample was weighed again. The signal of water profile of the specimen was immediately measured as well. All the measurements of the water profile were carried out with the same settings of the NMR equipment. In this study, the calibration was done within a short period (i.e. less than 2 h).

It is known that the increase of the NMR signal must be linear to the amount of absorbed water [33]. As shown in Fig. 3, in this experiment the increase of NMR signal of the specimen was linear to the amount of water absorbed by the specimen, indicating the NMR machine used in this study can quantify the amount of non-chemically bound water accurately.

3.4 Test procedures

Migration of extra water from the crack into the bulk cement paste during the process of autogenous self-healing can be monitored by NMR tests after the calibration of the equipment.

As illustrated in Fig. 4, at the start of the experiment the initial mass of the specimen was determined. The specimen was then placed into the NMR equipment and its initial water profile was measured. It took about 40 min for one NMR measurement. Then the specimen was taken away from the NMR equipment and the glass tube of the specimen was filled with water by using a syringe. When the glass tube was filled, the specimen was weighed again. After that the specimen was placed back to the NMR equipment for measuring the water profile again. By repeating these procedures, i.e., filling the glass tube, weighing the specimen and measuring the water profile, the amount of water absorbed by the bulk cement paste as a function of time was determined. The change of the

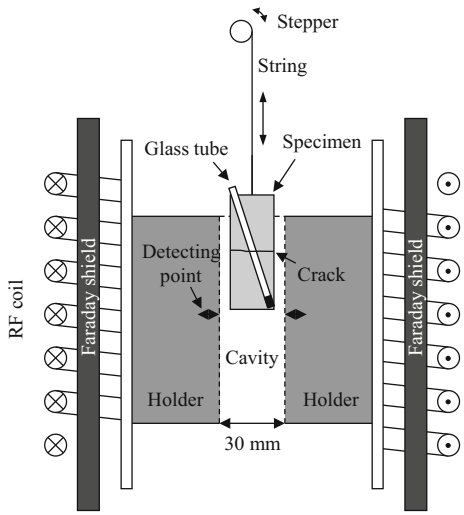

Fig. 2 A schematic diagram of the NMR setup

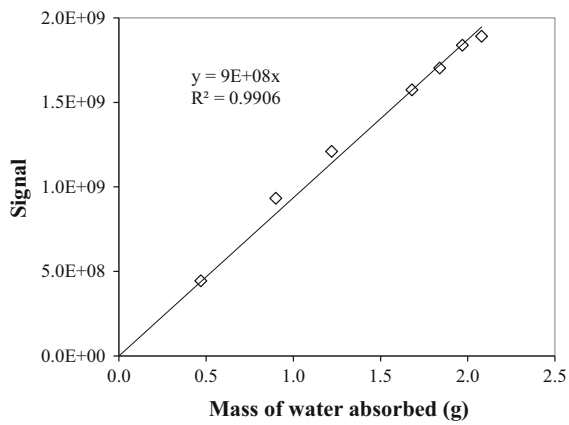

Fig. 3 Relationship between NMR signal and the mass of water absorbed by the sample

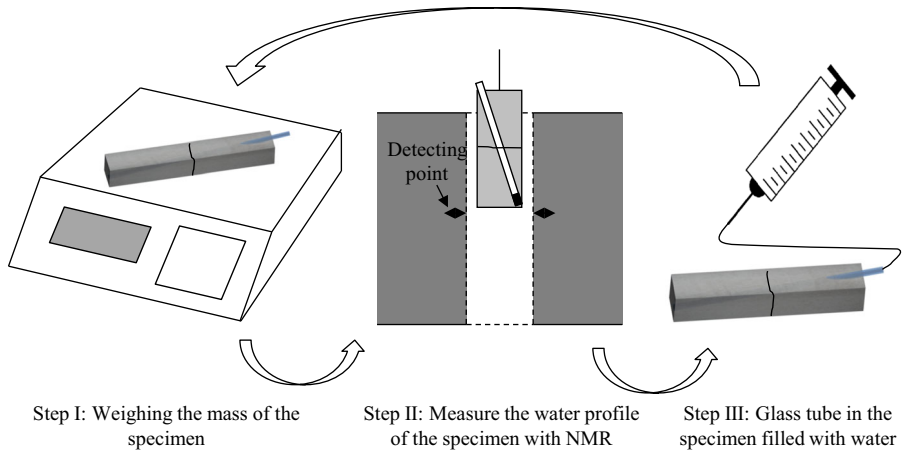

Fig. 4 A flow diagram of the experimental procedure

distribution of water within the specimen was monitored.

4 Experimental results and discussion

4.1 Water migration from the crack into bulk paste

Figure 5 shows the NMR signal profiles of the specimen at different periods of autogenous self-healing (from 0.0 to 22.0 h). As indicated in Sect. 3.1, by choosing the appropriate set of t_E and t_R (in Eq. 3) for the measurement, we can select to measure all the water present in gel and capillary pores or just the water present in the gel pores. Figure 5a represents the water in all the pores, while Fig. 5b only represents the water in gel pores. From the signal profile for $t = 0$ h (before the injection of water), it is found that water is distributed uniformly inside the specimen. As can be seen from the profile for $t = 0.7$ h, after water was injected into the glass tube, a sharp peak occurred at the position of the crack about 66 mm from the bottom of the specimen (the position of 0 corresponds to the bottom of specimen). It indicates that the injected water has penetrated into the crack and has started to migrate into the bulk paste. With increase of time, the intensity of the peak increased and the sharp fronts of the peak moved towards both ends of the specimen. It demonstrates that water migrated into the bulk paste from the crack and the water content of the cement paste nearby the crack increased significantly. After the glass tube had been fully filled with water for 5.0 h, the peak of the water profile measured in the region near the crack hardly increases (compare the water profile at 5.0 h with that at 22.0 h in Fig. 5a). In comparison, the fronts of the water profile still moved toward both ends of the specimen (see Fig. 5a, b). The intensity of NMR signal corresponding to gel pore (in Fig. 5b) is lower than that of NMR signal corresponding to all the pores (in Fig. 5a). When extra water penetrated into the cement paste, the increase of NMR signal for gel pore is similar to the increase of NMR signal for all the pores.

The increase of penetration depth of water with time is shown in Fig. 6. After 5 h (self-healing period), the penetration depth has reached a value of about 25 mm. During the time interval between the 5.0 and 70.0 h of autogenous self-healing, the penetration depth only increased by 15 mm. It is also interesting to note that in the first 2.0 h of autogenous self-healing the penetration depth in upward direction is similar to the value in downward direction. However, when the penetration time is larger than 5.0 h, the penetration depth in upward direction becomes smaller than that in downward direction. This can be contributed by the local variation of the microstructure. The gravity could also have some influence. However, its effect should be very small because the capillary force in the bulk paste is much larger than the gravity force of the pore solution.

4.2 A newly noticed phenomenon during autogenous self-healing: additional hydration taking place in the cement paste adjacent to the crack surfaces

Figure 7a shows that the fronts of water profile hardly move after 22-h exposure of the crack to water for

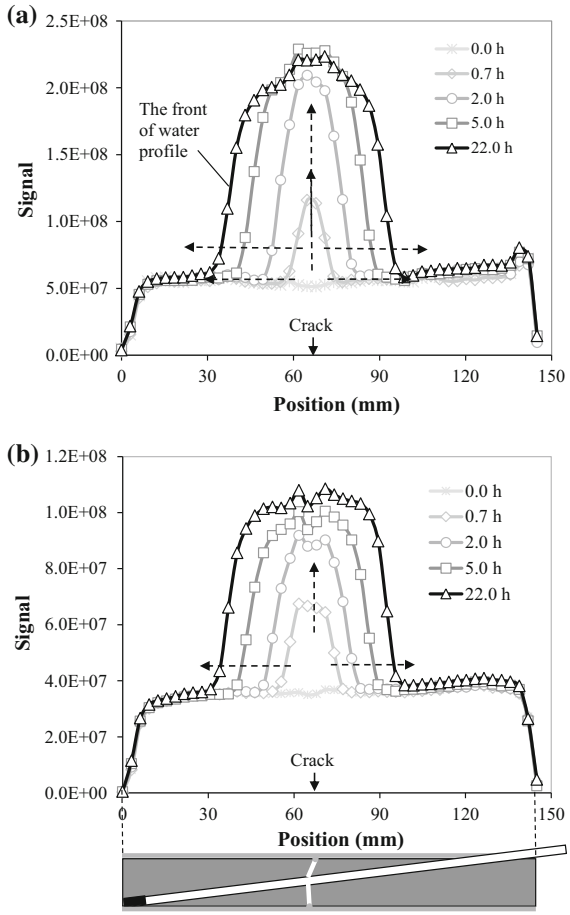

Fig. 5 NMR signal profiles after the supply of extra water for autogenous self-healing for different time until 22 h. The cracked specimen is made of cement paste with w/c ratio of 0.3. The supply of water starts at the age of 42 days of the specimen. **a** Signal for all the pores (capillary pores and gel pores) **b** signal for gel pores smaller than a specific radii (the specific radii was not quantified)

autogenous self-healing. Moreover, the peak of the water profile decreases with increase of time, which is different from that before 22 h (the peak of water profile increases before 22 h, as shown in Fig. 5a). In comparison, in the signal profiles for gel pores (Fig. 7b), the intensity does not decrease but even slightly increases. It should be mentioned that the glass tube remained filled with water during the test. It is not conceivable that there was a lack of water supply. The decrease of the NMR signal in Fig. 7a can be attributed to the decrease of the total porosity in the saturated region. A very slight increase of the NMR signal of gel pores in Fig. 7b suggests that additional gel has been formed in the bulk paste adjacent to the crack. It implies that capillary porosity decreases.

Note that in this experiment cement paste with a low w/c ratio of 0.3 was used. The degree of hydration of cement prior to the start of the tests is about 70 % at the age of 42 days, determined by modeling (the detailed information will be given in Sect. 5). Hence, there was still unhydrated cement left in the bulk paste due to the lack of water [39]. The extra water supplied via the tube promoted further hydration of the unhydrated cement particles in the bulk paste adjacent to the crack surfaces (as illustrated in Fig. 8).

4.3 Quantification of the extra water used for additional hydration of unhydrated cement

Figure 9 shows the amount of absorbed water measured with balances, compared with the extra water measured by NMR. In the beginning of the test (until $t = 5$ h), the amount of extra water in the specimen measured with balance was almost the same as that measured by NMR. However, after 5-h exposure of the crack to water for autogenous self-healing, the difference between these two groups of values became noticeable. As discussed in the previous section, further hydration of unhydrated cement particles in the bulk paste adjacent to the crack surfaces can be promoted by extra water coming from the crack. Therefore, a part of this extra water was used for further hydration of unhydrated cement particles in the bulk paste. Because the NMR equipment used in this test can only detect the non-chemically bound water inside the paste, the difference between the amount of absorbed water measured with balances and measured by NMR (see Fig. 9) indicates the transformation of non-chemically bound water into chemically bound water as a result of further hydration of the bulk paste. It should be mentioned that the difference between the amount of absorbed water measured with balances and measured by NMR is noticeable after 5-h healing time. It implies that the formation of hydration products takes place after 5-h healing time. Concentrations of ions in the pore solution decrease when extra water penetrates into the capillary pores from the crack. It takes some time for additional ions from dissolving cement particles to diffuse into the pore solution and make the pore solution become saturated with reaction products again. Further research is needed to explain this phenomenon.

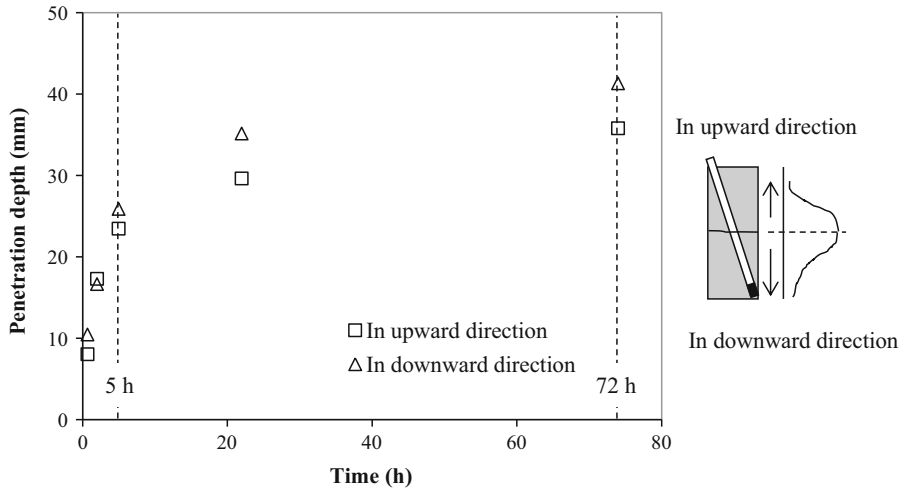

Fig. 6 Penetration depth of water from the crack to the bulk paste after the supply of extra water at different period of autogenous self-healing. The upward direction and downward direction is illustrated schematically. The cracked specimen is made of cement paste with *w/c* ratio is 0.3. The supply of water starts at the age of 42 days of the specimen

With the data in Fig. 9, the difference between the two groups of values, i.e. the amount of water consumed by further hydration can be determined. Figure 10 shows the amount of water used for further hydration in the bulk paste as a function of time. As discussed in Sect. 4.1, after 22-h exposure of the crack to water, the fronts of water profiles hardly moved. As illustrated in Fig. 10, the region of the bulk paste with extra water coming from the crack was determined by the fronts of water profile after 22-h exposure to water. The volume of cement paste in this region was calculated as 23.3 cm^3 ($2 \times 2 \times 6 - 3.14 \times (0.2)^2 \times 6$, excluding the volume of glass tube). As indicated in Fig. 10, after 216-h exposure of the crack to water, about 2.5 g of water is consumed for further hydration in the bulk paste in the aforementioned region.

4.4 Positions of additional hydration products: in the crack or in the capillary pores in the bulk paste?

As demonstrated by Huang et al. [26], in the process of autogenous self-healing, reaction products are formed in the crack. It is interesting to see how the filling of the crack with reaction products influences the NMR signal. As shown in Fig. 11, some sections of the specimen tested by NMR (indicated as measured sections) were intersected by the crack. In the measured sections intersected by the crack, not only the water in bulk paste, but also the water in the crack was measured. As self-healing of the crack proceeded, the space of the crack was filled with reaction products. This filling of the crack can also contribute to the decrease of the NMR signal. However, as explained in Fig. 11, in this test the distance between each measured section was 2.5 mm. Because the height difference between the highest position of the crack and the lowest position of the crack in the tested specimen was about 4 mm (see Fig. 11), there were only one or two measured sections intersected by the crack. It means that the filling of the crack can only affect one or two NMR signal reading. The decrease of NMR signal (in Fig. 7) measured in other sections is only due to the formation of hydration products in capillary pores, rather than in the crack.

5 Modeling of additional hydration of unhydrated cement adjacent to the crack surfaces

The experimental results present above indicates that some of the water coming from the crack was used for additional hydration of unhydrated cement particles in the bulk paste. However, these experimental data does not give detailed information of the evolution of microstructure adjacent to the crack surfaces. The aim of modeling in this section was to determine the evolution of microstructure of cement paste adjacent to the crack surfaces during the period of autogenous self-healing. To do so, the additional volume of hydration products caused by the extra water coming from the crack in the process of autogenous self-

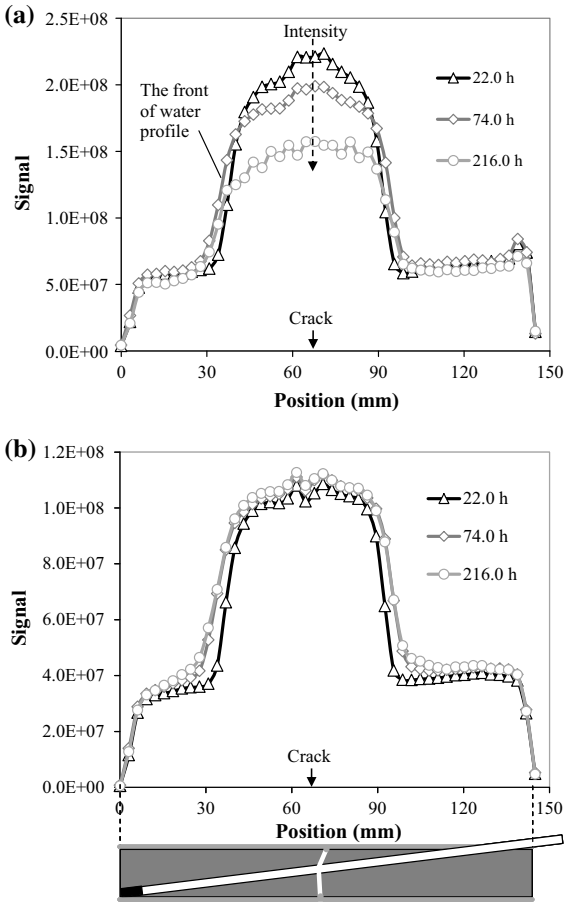

Fig. 7 NMR signal profiles after the supply of extra water (from 22 h to 216 h) for autogenous self-healing. The specimen is made of cement paste with w/c ratio is 0.3. The supply of water starts at the age of 42 days of the specimen. **a** Signal for all the pores (capillary pores and gel pores) **b** signal for gel pores smaller than a specific radii (the specific radii was not quantified)

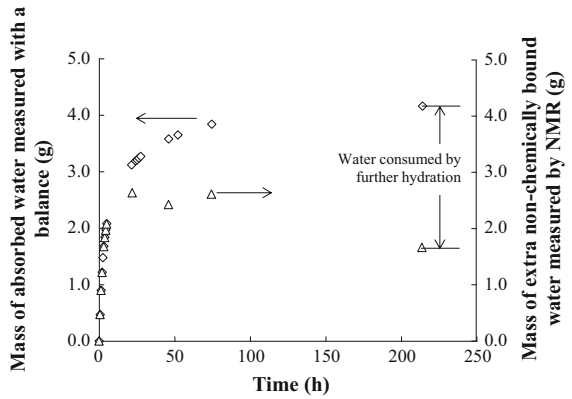

Fig. 9 Amount of absorbed water measured by a balance compared with the amount of non-chemically bound water measured by NMR. Time 0 refers to the beginning of the supply of extra water, which is from the age of 42 days of the cement paste

healing should be determined first. Figure 12 shows the flowchart of the simulation for calculating the additional volume of hydration products caused by the extra water coming from the crack in the process of autogenous self-healing, including three steps:

(1) Determine the volume fraction and mineral composition of cement in the bulk paste at the start of autogenous self-healing.
(2) Calculate the volume of cement that has reacted after the supply of water for autogenous self-healing.
(3) Calculate the volume of hydration products caused by the extra water coming from the crack during the process of autogenous self-healing.

By knowing the additional volume of hydration products caused by the extra water from the crack, the decrease of capillary porosity of cement paste after the additional hydration can then be calculated. Detailed information can be seen in subsections below.

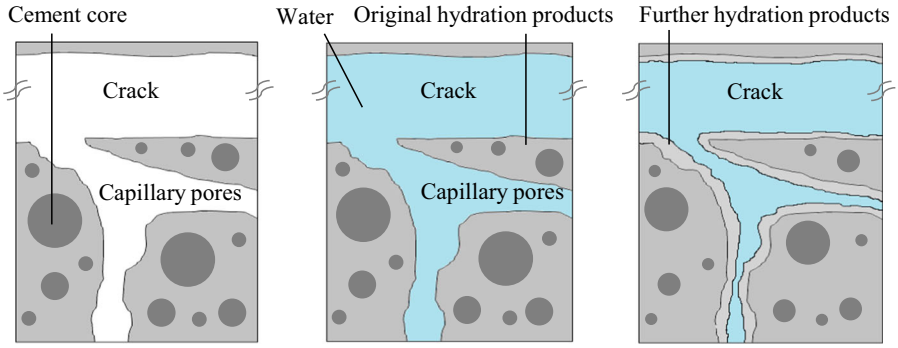

Fig. 8 Scheme of further hydration of unhydrated cement (in the cement paste adjacent to the crack surfaces) promoted by extra water coming from the crack in the process of autogenous self-healing

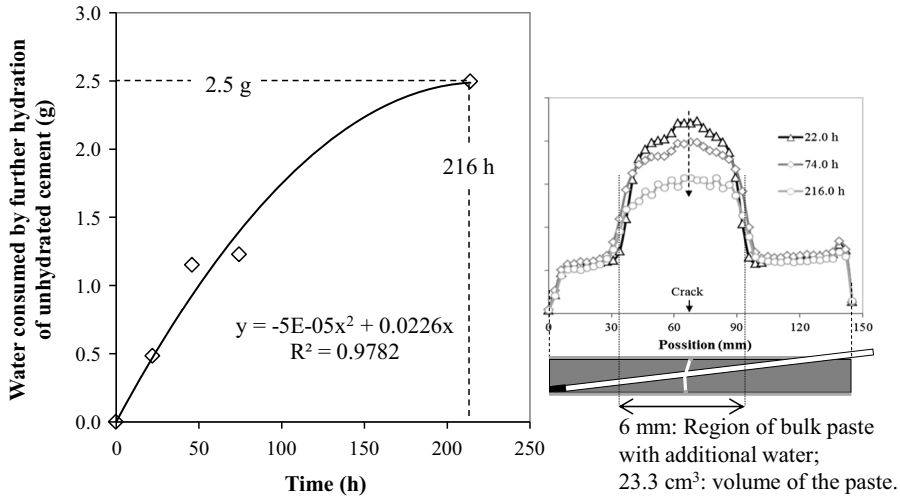

Fig. 10 Amount of extra water used for additional hydration of unhydrated cement in the bulk paste adjacent to the crack surfaces during the process of autogenous self-healing. The volume of cement paste with extra water is 23.3 cm^3

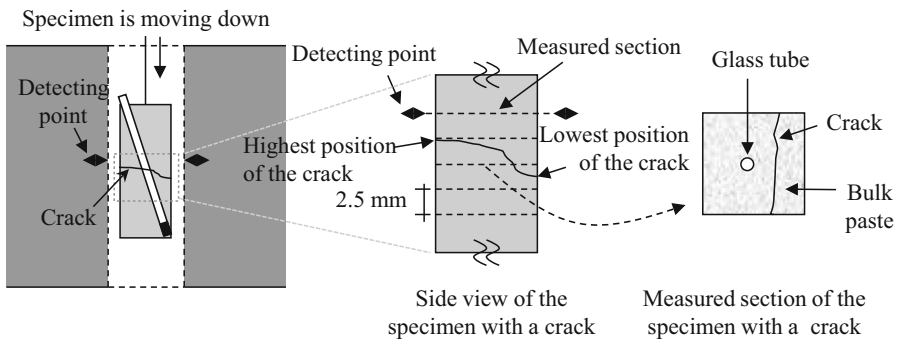

Fig. 11 A schematic diagram on the positions of measurements by NMR and the measured sections intersected by the crack

5.1 Mineral composition of cement in the bulk paste at the age of 42 days

In order to determine the volume fraction and mineral composition of cement in the bulk paste at the start of autogenous self-healing, the degrees of hydration of individual clinker components at the start of autogenous self-healing must be known. Parrot and Killoh's model [40] was used to simulate the hydration of individual clinker components. The hydration degree of each individual clinker component at the age of 42 days, i.e. at the start of autogenous self-healing, was calculated. From that information and the initial mineral composition of the cement CEM I 42.5 N in Table 2, the mineral composition of the cement that was left in the 42-day-old cement paste can be determined (see Table 3). The calculation showed that when $w/c = 0.3$, after 42 days the hydration speeds of C_3S, C_2S, C_3A and C_4AF were similar (see Fig. 13). In the simulation of further hydration of cement after the age of 42 days of the paste, it was assumed, therefore, that the speeds of further hydration of C_3S, C_2S, C_3A and C_4AF were the same.

5.2 Volume of cement that has reacted after supply of water for autogenous self-healing

As shown in Table 3, because all gypsum had been consumed at the age of 42 days, no more ettringite and AFm were formed during additional hydration of unhydrated cement. The reaction formulas of additional hydration of the remaining cement can be written as [41]:

$$C_3S + 5.3H \rightarrow C_{1.7}SH_4 + 1.3CH \quad (4)$$

$$C_2S + 4.3H \rightarrow C_{1.7}SH_4 + 0.3CH \quad (5)$$

$$C_3A + 6H \rightarrow C_3AH_6 \quad (6)$$

$$C_4AF + 10H \rightarrow C_3AH_6 + CH + FH_3 \quad (7)$$

Table 3 Mineral composition of Portland cement (CEM I 42.5 N, calculated with Bogue equation [45]) and the cement remaining in the bulk paste at the age of 42 days ($w/c = 0.3$, calculated with the approach of Parrot and Killoh [40])

Clinker component	C_3S	C_2S	C_3A	C_4AF	Calcite	Gypsum
Initial (wt.%)	64.1	13.0	7.9	8.1	4.4	4.2
At 42 days (wt.%)	17.2	5.7	2.6	3.6	2.5	0.0
Degree of hydration α (%)	73.2	56.2	67.1	55.6	43.2	100.0

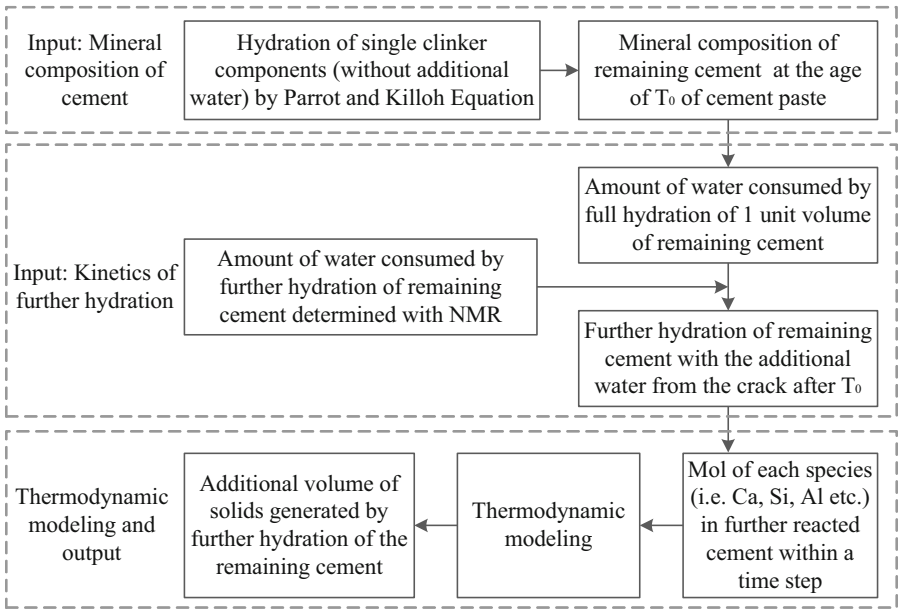

Fig. 12 Procedure of the simulation to calculate the additional volume of hydration products caused by the extra water coming from the crack during the process of autogenous self-healing

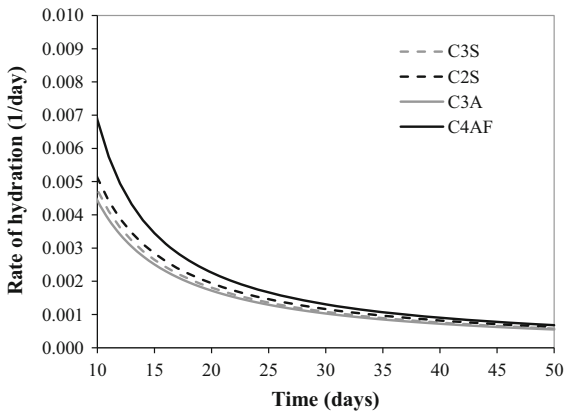

Fig. 13 Hydration speeds of individual clinker components in Portland cement paste, calculated with Parrot and Killoh's model. w/c ratio is 0.3

where C, S, H, A and F refers to CaO, SiO_2, H_2O, Al_2O_3 and Fe_2O_3, respectively.

Based on the mineral composition of remaining cement in the 42-day-old cement paste (Table 3) and the aforementioned reactions (Eqs. 4–7), the amount of water consumed by additional hydration of cement can be determined from the stoichiometry point of view. About 1.38 g of water was needed for full hydration of 1 cm^3 of cement that was left with the mineral composition listed in Table 3. Because the mass of water (M_w) used for additional hydration of cement in the bulk paste (23.3 cm^3) had been determined experimentally (see Fig. 10), the decrease of the volume of cement in the bulk paste was calculated: $M_w/1.38$ (see Fig. 14).

Figure 15 shows the degree of hydration of cement before and after the supply of extra water, compared with the results from back-scattered electrons (BSE) image analysis. For image analysis, seven samples were prepared. Three of them without supply of extra water were observed in ESEM at the age of 7, 14 and 42 days. Other four samples were supplied with extra water at the age of 42 days. When these samples were supplied with water for 24, 72, 96 and 216 h, respectively, their microstructures were observed in ESEM as well. For each sample, 45 images were taken. Degree of hydration of cement was calculated as the mean area fraction of unhydrated cement in the BSE image. Detailed information about determination of degree of hydration of cement referred to [42].

From Fig. 15, it was found that the degree of hydration calculated with the NMR data was consistent with the results from BSE image analysis. If there was no extra water penetrating into the cement paste, the hydration of cement hardly proceeded after the age of 42 days. This was due to the lack of water for the hydration. In the process of autogenous self-healing, extra water migrated into the bulk cement paste from the crack. The rate of further hydration of cement increased apparently. When cement paste had been supplied with water for autogenous self-healing for 216 h from the age of 42 days, the degree of hydration of the cement paste increased from 67 % to about 82 %, which was much higher than that for the case without extra water.

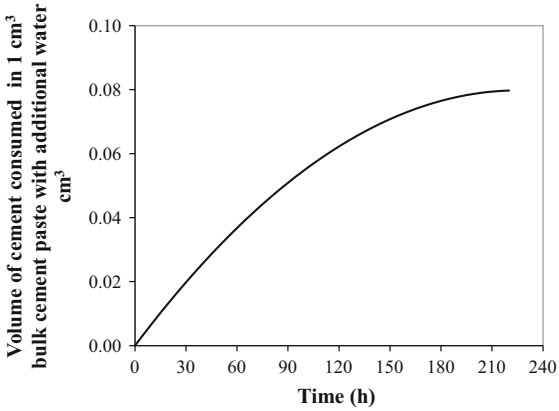

Fig. 14 Calculation of the volume of cement that has additionally reacted with the amount of extra water (coming from the crack).Time 0 is the beginning of the supply of extra water for autogenous self-healing, which is at the age of 42 days of the specimen. The initial *w/c* ratio of the cement paste is 0.3

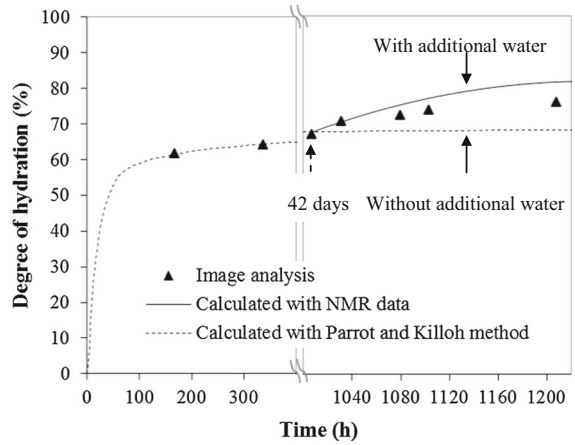

Fig. 15 Degree of hydration of cement paste with and without extra water coming from the crack, compared with results from BSE image analysis. Time 0 refers to the time when cement is mixed with water

5.3 Volume of hydration products caused by the extra water coming from the crack during the process of autogenous self-healing

With the volume of cement that had reacted with the extra water coming from the crack during the process of autogenous self-healing (see Fig. 14), the volumes of reaction products were calculated by using a thermodynamic model JCHESS van der Lee and de Windt [43].

The initial volume fraction of cement in cement paste before autogenous self-healing at the age of 42 days was about 16.5 % calculated with the degree of hydration presented in Fig. 15. As shown in Fig. 16, C–S–H was the main reaction product of the additional hydration caused by the extra water. Its volume accounted for more than 50 % of the total volume of the extra produced reaction products. Because calcite was still present in the cement paste at the age of 42 days (see Table 3), hemicarboaluminate was formed in the additional hydration. Its volume was slightly larger than that of portlandite. After 216-h autogenous self-healing of the crack, the total volume of reaction products caused by extra water was about two times the volume of cement that had reacted.

5.4 Evolution of the pore structure after additional hydration of unhydrated cement caused by extra water coming from the crack in the process of autogenous self-healing

Because the additional volume of reaction products after the supply of extra water was known (Fig. 16), the capillary porosity after additional hydration of cement paste can be determined when the initial capillary porosity before autogenous self-healing has been determined.

Figure 17 presents the capillary porosity of the cement paste with and without extra water. The capillary porosity hardly changed after the age of 42 days of the cement paste if no extra water was supplied. This was consistent with the kinetics of hydration presented in Fig. 15. The capillary porosity decreased significantly if extra water migrated into the cement paste from the crack (see Fig. 17). After 216-h autogenous self-healing from the age of 42 days of cement paste, the capillary porosity of the cement paste adjacent to the crack surfaces was less than 4 %.

However, after 216-h autogenous self-healing there was hardly any further decrease of capillary porosity of the cement paste adjacent to the crack surfaces. As shown in Fig. 18, the NMR signal of the specimen with water in the crack for autogenous self-healing for 360 h was very similar to the signal of the specimen

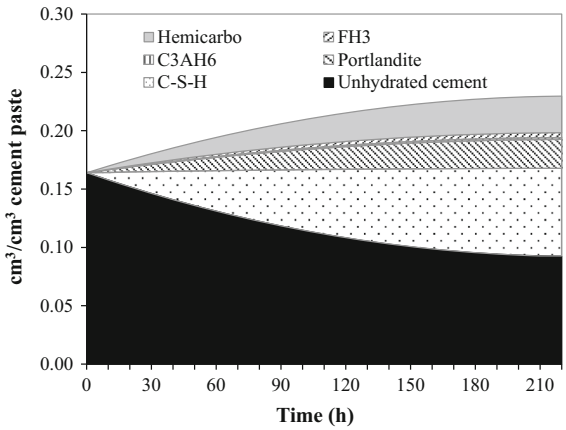

Fig. 16 Volume of hydration products caused by extra water coming from the crack after autogenous self-healing, determined by means of thermodynamic modeling. Time 0 is the beginning of autogenous self-healing, i.e. the supply of water, which is at the age of 42 days of the specimen. "Hemicarbo" refers to hemicarboaluminate

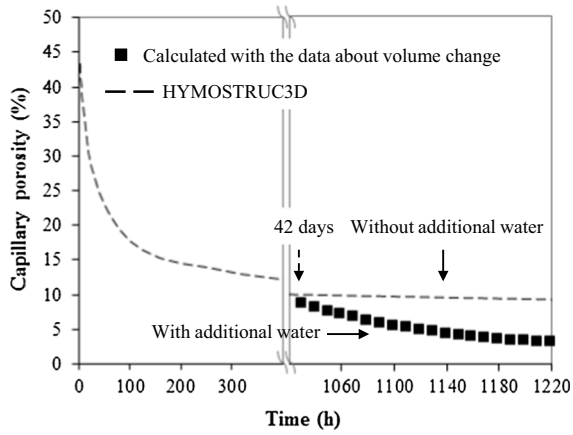

Fig. 17 Capillary porosity of cement paste with extra water coming from the crack, compared to that if no extra water is supplied. For the supply of additional water, it starts at the age of 42 days of the cement paste. The initial *w/c* ratio of the cement paste is 0.3

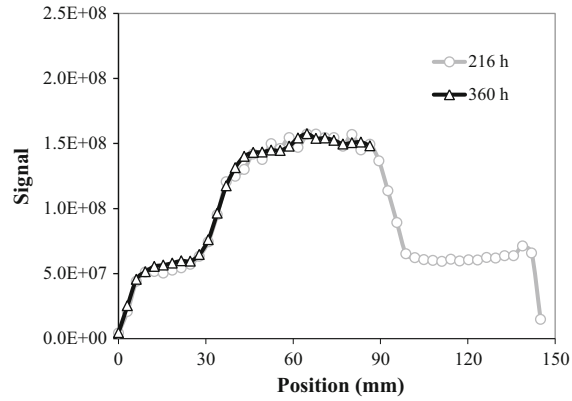

Fig. 18 NMR signal profiles of the specimen after autogenous self-healing for 216 h, compared with that for 360 h. The supply of water for autogenous self-healing begins at the age of 42 days of the specimen. The signal corresponds to all the pores. Because the specimen was broken when it had been supplied with water for autogenous self-healing for 360 h, only a part of it was tested

with extra water in the crack for 216 h (only a part of the specimen was tested because it was broken when it had been supplied with water for autogenous self-healing for 360 h). It also suggested that the capillary porosity of the cement paste adjacent to the crack surfaces hardly decreased after autogenous self-healing for 216 h. This was consistent with the result in Fig. 17. From the calculation in this section, it can be learned that the microstructure of cement paste

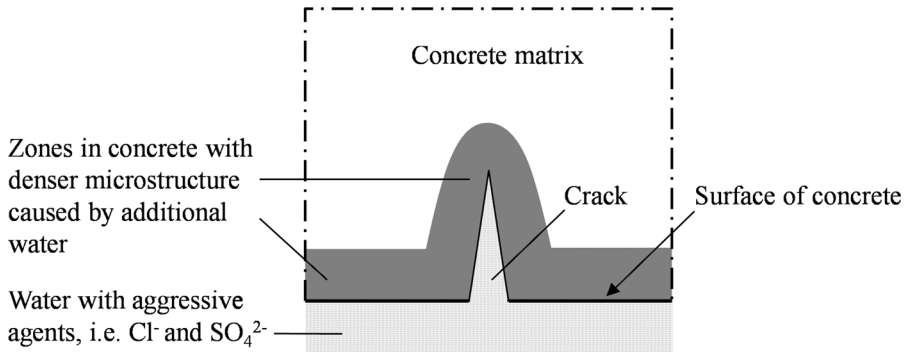

Fig. 19 Schemes for illustrating the effect of absorption of water by the bulk paste on the densification of microstructure of the bulk paste and on autogenous self-healing of the crack

adjacent to the crack surfaces becomes much denser after autogenous self-healing.

6 Discussion

This study shows that in the process of autogenous self-healing the water in the crack migrated into concrete made of low w/c ratio through the crack surfaces. A layer of the bulk paste adjacent to the crack surfaces became much denser because of additional hydration of unhydrated cement with the extra water coming from the crack (schematically shown in Fig. 19). The densification of microstructure adjacent to the crack, on the one hand, decreased the diffusion of reaction products from the bulk paste into cracks and had, therefore, a negative effect on filling of the crack with reaction products. On the other hand it will decrease the ingress of aggressive agents into the bulk concrete matrix and prolong the service life of concrete structures. The densification of the cement paste adjacent to the crack surfaces is actually independent with the crack width. It means that even though a crack with a large width was not completely filled with reaction products after autogenous self-healing, the ingress of aggressive agents into the bulk concrete matrix will be still difficult.

Before this study, in term of autogenous self-healing only the recoveries that related to the filling of cracks were concerned. This study provides a new insight into autogenous self-healing. Moreover, this study also gives implies to external curing of concrete. If water is allowed to penetrate into concrete matrix through the surface of the matrix from the outside environment, a layer of dense cement paste can be formed adjacent to the matrix surface as well. As a result, the inner material of the matrix can be protected, which is in good agree with [44].

7 Conclusions

Nuclear magnetic resonance (NMR) technique was utilized to investigate water migration from cracks into the bulk paste during the process of autogenous self-healing. The changes of water content and water distribution in the bulk paste adjacent to the crack surfaces were quantified by NMR. From the experimental study, it was noticed that additional hydration taking place in the cement paste adjacent to the crack surfaces during the process of autogenous self-healing. Densification of the cement paste adjacent to the crack surfaces was determined by means of modelling. The following conclusions can be drawn:

- When water penetrates into the cement paste (water to cement ratio of 0.3 at the age of 42 days) from a crack, NMR signal for all the pores in the paste adjacent to the crack increases first and then decreases.
- The decrease of water content in cement paste being supplied with water indicates that some of the extra water was used for additional hydration of unhydrated cement particles in the bulk paste.
- Additional hydration of unhydrated cement with extra water makes the cement paste adjacent to the crack surfaces become much denser. When a crack of cement paste was exposed to water at the age of 42 days for 216 h, the capillary porosity of the paste adjacent to the crack surfaces decreases to less than 4 %.
- Before this study, in term of autogenous self-healing only the recoveries that related to the

filling of cracks were concerned. The observation of densification of cement paste adjacent to the crack surfaces provides a new insight into autogenous self-healing.

Acknowledgments The authors would like to thank the National Basic Research Program of China (973 Program: 2011CB013800), National Nature Science Fund (51178104) and the China Scholarship Council (CSC) for the financial support. Mrs Jingping Han's help on the NMR experiments is also appreciated.

References

1. van Breugel K (2012) Self-healing material concepts as solution for aging infrastructure. In 37th conference on our world in concrete & structures, Singapore
2. Dry CM (2000) Three designs for the internal release of sealants, adhesives, and waterproofing chemicals into concrete to reduce permeability. Cem Concr Res 30(12):1969–1977
3. Ramachandran SK, Ramakrishnan V, Bang SS (2001) Remediation of concrete using micro-organisms. ACI Mater J 98:3–9
4. Ahn TH, Kishi T (2010) Crack self-healing behavior of cementitious composites incorporating various mineral admixtures. J Adv Concr Technol 8(2):16
5. Joseph C, Jefferson A, Isaacs B, Lark R, Gardner D (2010) Experimental investigation of adhesive-based self-healing of cementitious materials. Mag Concr Res 62(11): 831–843
6. Van Tittelboom K, De Belie N, Van Loo D, Jacobs P (2011) Self-healing efficiency of cementitious materials containing tubular capsules filled with healing agent. Cem Concr Compos 33(4):497–505
7. Wiktor V, Jonkers HM (2011) Quantification of crack-healing in novel bacteria-based self-healing concrete. Cem Concr Compos 33(7):763–770
8. Wang J, Van Tittelboom K, De Belie N, Verstraete W (2012) Use of silica gel or polyurethane immobilized bacteria for self-healing concrete. Constr Build Mater 26(1):532–540
9. de Rooij MK, Tittelboom Van, De Belie N, Schlangen E (2013) Self-healing phenomena in cement-based materials. Springer, New York
10. Soroker VJ, Denson AJ (1926) Autogenous healing of concrete. Zement 25(30):76
11. Brandeis F (1937) Autogenous healing of concrete. Beton u Eisen 36(12):11
12. Hearn N (1998) Self-sealing, autogenous healing and continued hydration: what is the difference? Mater Struct 31(8):563–567
13. Hyde GW, Smith WJ (1889) Results of experiments made to determine the permeability of cements and cement mortars. J Frankl Inst Phila 128:199–207
14. Glanville WH (1931) The permeability of Portland cement concrete. Build Res Tech Pap 3:1–61
15. Sahmaran M, Keskin SB, Ozerkan G, Yaman IO (2008) Self-healing of mechanically-loaded self consolidating concretes with high volumes of fly ash. Cem Concr Compos 30(10):872–879
16. Van Tittelboom K, Gruyaert E, Rahier H, De Belie N (2012) Influence of mix composition on the extent of autogenous crack healing by continued hydration or calcium carbonate formation. Constr Build Mater 37:349–359
17. Lv Z, Chen H (2013) Self-healing efficiency of unhydrated cement nuclei for dome-like crack mode in cementitious materials. Mater Struct 46:1–12
18. Yang Y, Lepech MD, Yang E-H, Li VC (2009) Autogenous healing of engineered cementitious composites under wet-dry cycles. Cem Concr Res 39(5):382–390
19. Qian S, Zhou J, de Rooij MR, Schlangen E, Ye G, van Breugel K (2009) Self-healing behavior of strain hardening cementitious composites incorporating local waste materials. Cem Concr Compos 31(9):613–621
20. Granger S, Loukili A, Pijaudier-Cabot G, Chanvillard G (2007) Experimental characterization of the self-healing of cracks in an ultra high performance cementitious material: mechanical tests and acoustic emission analysis. Cem Concr Res 37(4):519–527
21. Ter Heide N (2005) Crack healing in hydrating concrete. Msc, Delft University of Technology, Delft
22. Edvardsen C (1999) Water permeability and autogenous healing of cracks in concrete. ACI Mater J 96(4):448–454
23. Reinhardt H-W, Jooss M (2003) Permeability and self-healing of cracked concrete as a function of temperature and crack width. Cem Concr Res 33(7):981–985
24. Hearn N, Morley C (1997) Self-sealing property of concrete-experimental evidence. Mater Struct 30(7):404–411
25. Schlangen E, Ter Heide N, van Breugel K (2006) Crack healing of early age cracks in concrete. In: Konsta-Gdoutos MS (ed) Measuring, monitoring and modeling concrete properties. Springer, Netherlands
26. Huang H, Ye G, Damidot D (2013) Characterization and quantification of self-healing behaviors of microcracks due to further hydration in cement paste. Cem Concr Res 52:71–81
27. Jacobsen S, Sellevold EJ (1996) Self healing of high strength concrete after deterioration by freeze/thaw. Cem Concr Res 26(1):55–62
28. Li VC, Yang E-H (2007) Self-healing in concrete materials. In: van der Zwaag S (ed) Self healing materials an alternative approach to 20 centuries of materials science. Springer, Dordrecht
29. Huang H, Ye G, Damidot D (2014) Effect of blast furnace slag on self-healing of microcracks in cementitious materials. Cem Concr Res 60:68–82
30. Callaghan PT (1991) Principles of nuclear magnetic resonance microscopy. Clarendon Press, Oxford
31. Blumich B (2000) NMR imaging of materials. Oxford Science Publications, New York
32. Hazrati K, Pel L, Marchand J, Kopinga K, Pigeon M (2002) Determination of isothermal unsaturated capillary flow in high performance cement mortars by NMR imaging. Mater Struct 35(10):614–622
33. Valckenborg R, Pel L, Hazrati K, Kopinga K, Marchand J (2001) Pore water distribution in mortar during drying as determined by NMR. Mater Struct 34(10):599–604

34. Friedemann K, Stallmach F, Kärger J (2006) NMR diffusion and relaxation studies during cement hydration—a non-destructive approach for clarification of the mechanism of internal post curing of cementitious materials. Cem Concr Res 36(5):817–826
35. Kimmich R (1997) NMR tomography, diffusometry, relaxometry. Springer, Heidelberg
36. McDonald PJ, Mitchell J, Mulheron M, Monteilhet L, Korb JP (2007) Two-dimensional correlation relaxation studies of cement pastes. Magn Reson Imaging 25(4):470–473
37. Kopinga K, Pel L (1994) One-dimensional scanning of moisture in porous materials with NMR. Rev Sci Instrum 65(12):3673–3681
38. Pel L (1995) Moisture transport in porous building materials. Ph.D, Eindhoven University of Technology
39. Powers TC, Brownyard TL (1948) Studies of the physical properties of hardened Portland cement paste (9 parts), J Am Concr Inst 43, Bulletin 22, Chicago
40. Parrot LJ, Killoh DC (1984) Prediction of cement hydration. Br Ceram Proc 35:41–53
41. Taylor HFW (1997) Cement chemistry. Thomas Telford Publishing, London
42. Ye G (2003) Experimental study and numerical simulation of the development of the microstructure and permeability of cementitious materials. PhD, Delft University of Technology
43. van der Lee J, de Windt L (1999) "CHESS." from http://chess.geosciences.ensmp.fr/
44. Liu J, Xing F, Dong B, Ma H, Pan D (2014) Study on water sorptivity of the surface layer of concrete. Mater Struct 47(11):1941–1951
45. Bogue RH (1955) The chemistry of Portland cement. Reinhold Pub. Corp, New York